Pergamon

Int. J. Heat Mass Transfer. Vol. 38, No. 12, pp. 2169–2174, 1995

0017-9310/95 $9.50+0.00

0017-9310(94)00339-4

The effect of natural convection in mass transport measurements in dilute liquid alloys

J. P. GARANDET, C. BARAT and T. DUFFAR

Commissariat à l'Energie Atomique, DTA/CEREM/DEM/SES, Centre d'Etudes Nucléaires de Grenoble, 38054 Grenoble Cedex 9, France

(*Received* 1 *October* 1993 *and in final form* 30 *October* 1994)

Abstract—A coupled scaling analysis–numerical simulation approach is carried out in order to quantify the effect of natural convection on the accuracy of diffusion coefficient measurements in dilute liquid alloys. This effect is seen to scale with the square of the product of the Grashof and Schmidt numbers. Our results also indicate that the design of the experimental set-up should be optimized, especially in the case of species such as liquid metal components, that often have low diffusion coefficients. The possibility of damping convection in electrically conducting fluids by means of an externally applied magnetic field is also briefly discussed.

I. INTRODUCTION

The knowledge of solute diffusion coefficients is of primary importance in a variety of processes, including crystal growth from the melt and solidification [1]. Besides, there is also a need for accurate data in order to determine which of the various theories of atomic transport, e.g. the "quasicrystalline" and "free volume" models [1, 2], are applicable. However, measurements are not easy to perform since natural convection, hardly avoidable in practice, may interfere with the diffusive fluxes. In this sense microgravity experiments offer a very interesting—but costly—alternative [3, 4].

In a typical experimental long capillary or shear cell set-up [1], the development of an initial one-dimensional concentration step is followed over time. On Earth, thin vertical capillaries under a stabilizing temperature gradient are generally used to limit convective solute transport. After completion of the experiment, the composition in the resulting solid alloy is measured and fitted by a Gaussian error function under the assumption that the diffusion coefficient is concentration independent.

A standard procedure is to take a compositional average over slices normal to the capillary axis. In some cases though, the lateral variations are characterized, and the degree of radial segregation was proposed as a diagnostic to account for the convective effects in the liquid phase [2]. Intuitively, one would expect that the sensitivity of a given experiment to convection will be higher for the case of species with low diffusivities, but a simple criterion is still lacking.

To address these points and to gain some insight into the physics of the mass transfer process, we relied on a coupled numerical–scaling analysis approach. The purpose of this paper is to understand the relevant transport mechanisms and to propose a quantitative first estimate of the effect of convection in ground based diffusion coefficient measurements in order to assess them as candidates for space experiments.

II. BACKGROUND

In this section, we shall first present the hypotheses and then proceed to show how a dimensional analysis can be used to identify the relevant variables. We model the actual, cylindrical geometry using an idealized, two-dimensional planar cell, shown schematically in Fig. 1. The mass transfer equation is written as:

$$\partial C/\partial t+(\mathbf{V}\cdot\nabla)C = D\nabla^2 C \qquad (1)$$

where D is the diffusion coefficient and $\mathbf{V}$ is the fluid velocity. As an initial condition, we assume that the diffusion couple is homogenized before the beginning of the experiments:

$$t=0 \quad C=C_0 \quad Z\leqslant L/2 \quad C=C_1 \quad Z>L/2.$$

The associated boundary conditions are as follows:

top/bottom walls	$\partial T/\partial Z=0$	$\partial C/\partial Z=0$
left wall	$T=T_0$	$\partial C/\partial X=0$
right wall	$T=T_0+\Delta T_H$	$\partial C/\partial X=0.$

Since the capillary is vertical, buoyancy is governed by the interaction of gravity and horizontal density gradients. Only weak convection will be considered in this paper, since we focus on small perturbations of the mass transfer process. For low Prandtl number fluids, such as metals or semiconductors, the ratio of thermal to solutal diffusivity is very high and weak

NOMENCLATURE

B	applied magnetic field
C	alloy composition
C_0, C_1	end concentrations of the diffusing couple
D	actual diffusion coefficient
D^*	apparent diffusion coefficient
$\bar{G}$	maximum vertical concentration gradient
G_L	vertical concentration gradient in the left part of the cavity
G_R	vertical concentration gradient in the right part of the cavity
g_0	intensity of gravity
H, L	width and length of the cavity
t_d	duration of the simulated experiment
$\mathbf{V}$	velocity vector
W	vertical velocity component
X, Z	horizontal and vertical coordinates.

Greek symbols

β_T	thermal expansion coefficient
ΔC_H	maximum lateral concentration variation
ΔT_H	lateral temperature variation
$\bar{\delta}$	length scale of established vertical concentration gradient
ε	aspect ratio of the cavity, H/L
η	dynamic viscosity of the fluid
ν	kinematic viscosity of the fluid
σ	electrical conductivity of the fluid
τ	non-dimensional experiment duration, $(Dt_d)^{1/2}/L$.

Non-dimensional numbers

Gr	Grashof number, $= \beta_T g_0 \Delta T_H H^3/\nu^2$
Ha	Hartmann number, $= B\,H\,(\sigma/\eta)^{1/2}$
Sc	Schmidt number, $= \nu/D$.

convection (by solute transport standards) should not affect the heat flow. A constant lateral temperature gradient is thus expected between the side walls, but this point will be checked numerically.

In dilute alloys, the lateral concentration differences are generally very low, due to both the assumed weakness of the flow and the small absolute composition range of the diffusing couple. Thus, their effect on density variations can often be safely neglected, so that only the lateral temperature differences need be considered. However, this assumption can be checked *a posteriori* from a comparison of the thermal and solutal driving forces.

Consistent with our low convective level hypothesis, the fluid velocity should then scale with the Grashof number [3], $Gr = \beta_T g_0 \Delta T_H H^3/\nu^2$. In the above expression, β_T is the thermal expansion coefficient, g_0 the gravity level, ν the kinematic viscosity, H the lateral dimension of the capillary and ΔT_H a measure of the horizontal temperature difference. It should be kept in mind that the fluid velocity may scale with $Gr^{1/2}$ at high convective levels [5], but this only occurs for values of the Grashof number far greater than those considered in the present work.

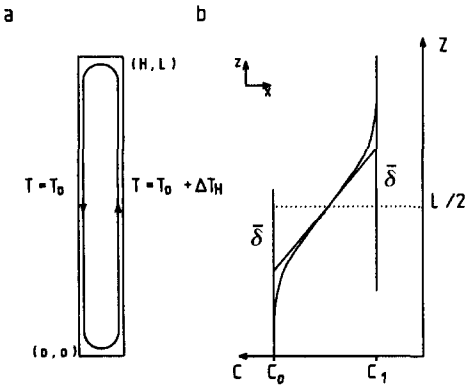

Fig. 1. Model cavity with coordinates axis (a) and typical axial composition profile (b). The composition gradient is established over a length scale $\bar{\delta}$ measured from the middle of the cavity ($Z = L/2$)

From the proportionality relation between $\mathbf{V}$ and Gr, it can be easily shown [6] that convective mass transport scales with the product of the Grashof and Schmidt ($Sc = \nu/D$) numbers. From dimensional analysis arguments, the problem is also seen to depend on two other groups, namely the aspect ratio of the cavity $\varepsilon = H/L$ and the scale of the experiment duration, $\tau = (Dt_d)^{1/2}/L$, t_d being the dimensional diffusion time.

The sensitivity of a given experiment to convection will certainly vary with the $Gr \times Sc$ product, but an influence of ε and τ can be expected *a priori*, since both L and t_d affect the resulting composition profile. We shall now proceed to test these assumptions using a coupled scaling analysis–numerical simulations approach.

III. SCALING ANALYSIS

Our purpose in this section is to estimate the order of magnitude of the diffusion and convection terms appearing in equation (1). We shall only briefly recall the principles of the scaling procedure; for more information on these matters, the interested reader is referred to Bejan [5]. The key idea is that the derivatives can be approximated from *a priori* defined ranges of variation. For instance, if the composition is assumed to increase smoothly from C_A in Z_A to C_B

in Z_B, the concentration gradient over the interval $[Z_A, Z_B]$ will be given as $\partial C/\partial Z \simeq (C_A - C_B)/(Z_A - Z_B)$.

This may appear as a drastic simplification, but this kind of approach was shown to be very fruitful in the fields of heat and mass transfer (see for instance refs. [5–7]). In the present problem, we shall proceed to estimate the diffusive and convective contributions in the laterally averaged equation (1) in order to identify the dominant transport mode.

Convective contribution

Since the fluid velocity is expected to be parallel to the Z-axis, except in the areas where the composition is uniform, the convective term in equation (1) can be approximated as: $(\mathbf{V}\cdot\nabla)C \simeq W\,\partial C/\partial Z$, where W is the vertical velocity component. Now if the concentration gradient $\partial C/\partial Z$ does not depend on lateral position, the no net flow condition yields:

$$\int_0^H W\,\partial C/\partial Z\,\mathrm{d}X = \partial C/\partial Z \int_0^H W\,\mathrm{d}X = 0.$$

Thus, the convective effects could not be observed. Since an effect is present, the lateral variations of the concentration gradient along the Z-axis must be accounted for.

On physical grounds, we rely on the fact that the lateral solute segregation can be related to the main features of the velocity field [7]. After some simple but tedious algebra (see Appendix for details), the absolute value of the integral of the convection term in equation (1) around the locations $Z = L/2 \pm \bar{\delta}$ can be estimated as:

$$\int_0^H W\,\partial C/\partial Z\,\mathrm{d}X = \frac{1}{4}\frac{H^3 \bar{W}^2}{D\bar{\delta}}|\vec{G}| \qquad (2)$$

$\bar{W}$ and $|\vec{G}|$ being, respectively, the average convection velocity across the cavity and the absolute value of the maximum composition gradient along the Z-axis, i.e. at $Z = L/2$.

Diffusive contribution

The estimation is here much simpler; indeed, from the no flux condition ($\partial C/\partial X = 0$ for $X = 0$ and $X = H$), the integration of the Laplacian term in equation (1) yields:

$$D\int_0^H \nabla^2 C\,\mathrm{d}X = D\int_0^H \partial^2 C/\partial Z^2\,\mathrm{d}X. \qquad (3)$$

To the first order, the average composition gradient along the Z-axis varies from $\vec{G}$ to 0 over a length scale $\bar{\delta}$ (see Fig. 1), so that $\partial^2 C/\partial Z^2 = -\vec{G}/\bar{\delta}$ for $Z \in [L/2, L/2+\bar{\delta}]$ and $\partial^2 C/\partial Z^2 = \vec{G}/\bar{\delta}$ for $Z \in [L/2-\bar{\delta}, L/2]$. The absolute value of the Laplacian term in equation (3) around the locations $Z = L/2 \pm \bar{\delta}$ is thus given as:

$$D\int_0^H \partial^2 C/\partial Z^2\,\mathrm{d}X = \frac{DH}{\bar{\delta}}|\vec{G}|. \qquad (4)$$

Comparing equations (2) and (4), the ratio of the convective and diffusive mass transfer contributions is:

$$R = \tfrac{1}{4}H^2\frac{\bar{W}^2}{D^2}. \qquad (5)$$

From the Birikh profile [8], we get $\bar{W} = \nu/H\,Gr/192$ and equation (5) finally becomes

$$R(\%) \simeq (Gr\,Sc)^2/1500. \qquad (6)$$

IV. NUMERICAL SIMULATION

In parallel with the scaling analysis, we also performed numerical simulations of the mass transfer problem. Equation (1) was thus solved with the help of the FIDAP finite elements code, implemented on an HP 730 workstation. Typical mesh dimensions were 26×3 (nine-nodes quadrilateral elements). We made sure that the final results did not depend on both space and time discretizations. We chose a successive substitution method, with implicit time scheme, to obtain the solution. The classical Boussinesq approximation was used in the Navier–Stokes equation.

Equation (1) being linear in concentration, all the computations were made with $C_0 = 1$ and $C_1 = 0$. A typical output of the program is shown in Fig. 2. After completion of the simulated run, we took the lateral composition average at the nodes located in the Z-direction. The apparent diffusion coefficient D^* was then estimated from an error function best fit of this composition average and compared to the exact value D used as an input in the transport equation.

We checked that convection did not modify the thermal field with respect to the reference, pure

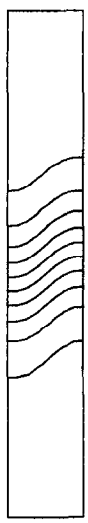

Fig. 2. Isoconcentration lines obtained from a FIDAP simulated run for the case $Gr \times Sc = 360$ (lateral magnification $\times 10$).

diffusion case ($\Delta T_H = 0$) and that the maximum velocity in the fluid did indeed scale with the Grashof number. Moreover, the convective field was seen to remain directed along the Z-axis except in small recirculating regions [9] and to compare well with Birikh's one-dimensional solution [8].

Even under perturbed conditions, the concentration profile kept an error function appearance; however, when convection was too intense, the composition field became homogeneous, meaning that no fit was possible ('infinite' apparent diffusion coefficient). In some cases the lateral concentration variations were quite high ($\Delta C_H/\bar{C} \simeq 15\%$), but still we obtained good estimates of D (relative error $D^*/D-1 \simeq 0.5\%$). Thus, it appears that lateral segregation is not a good indicator of the effect of convection in the present problem.

We also observed the evolution of the length scale $\bar{\delta}$ over which the concentration gradient along the Z-axis is established (see Fig. 1): under purely diffusive conditions, $\bar{\delta}$ followed a $(Dt)^{1/2}$ scaling law. With significant convection, the same scaling law was seen to hold, with D^* replacing D. It thus seems that an *a priori* correct composition profile (i.e. without obvious perturbations) at the end of the experiment does not guarantee the validity of the measurement.

A variety of runs were simulated in the course of this work. Experimental conditions and results in terms of induced error $D^*/D-1$ (in percent) are summarized in Table 1. It is clear that both the aspect ratio of the cavity and the experiment duration have no influence on the accuracy of the measurement at a given value of $Gr \times Sc$, even though $\bar{\delta}$ does increase with time. The $Gr \times Sc$ dependence is parabolic, as can be seen in Fig. 3, and can be fitted as $D^*/D-1(\%) = (Gr \times Sc)^2/4050$.

V. DISCUSSION

As seen in equation (6), the relative convective transport contribution in the laterally averaged mass transport equation features the square of the $Gr \times Sc$ product. On the other hand, lateral segregation is proportional to the fluid velocity. The two phenomena have different scaling laws and as a consequence radial segregation can not be taken as a relevant measure of the effect of convection.

Table 1. Non-dimensional parameters used in the numerical simulations and resulting errors in terms of diffusion coefficient

ε	τ	$Gr\,Sc$	$(D^*-D)/D$ (%)
7.5×10^{-3}	3.5×10^{-2}	360	32
	8.5×10^{-2}		32.5
3.75×10^{-3}	3.5×10^{-2}	360	31.5
7.5×10^{-3}			32
1.5×10^{-2}			32
7.5×10^{-3}	3.5×10^{-2}	9	0
		45	0.5
		90	2
		180	8
		270	18.5
		360	32
		450	50

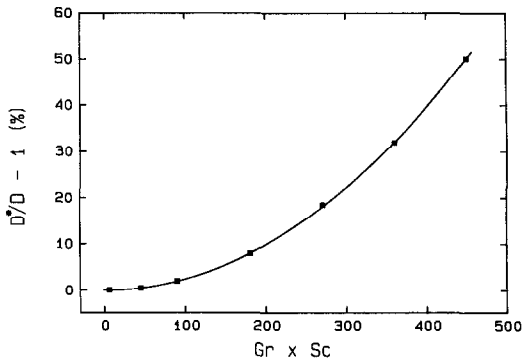

Fig. 3. Variation of the error in diffusion coefficient (%) due to natural convection effects.

Another result of the scaling analysis is that $\bar{\delta}$ does not appear in equation (5). This means that, even though the composition profile changes with time, its sensitivity to convection is not affected by the duration of the experiment, at least when the end concentrations remain close to their initial values. Finally, it is also clear that equation (5) predicts no effect of the aspect ratio of the cavity.

Scaling analysis and numerical results thus lead to similar conclusions, and we have to admit that the sensitivity of a given measurement to convection only depends on the value of the $Gr \times Sc$ product. Moreover, let us suppose that the additional convective contribution can be simply added to the diffusive term,

$$D^* = D(1+R) \tag{7}$$

the ratio R being defined in equation (5). The error in terms of $D^*/D-1$ is then equal to R and the values coming from the numerical fit (4050) and the scaling analysis (1500) are thus in good order of magnitude agreement.

Apparently, since Gr varies with the third power of H, reducing the capillary dimensions will guarantee nearly purely diffusive transport, in particular because in real experimental set-ups the lateral temperature difference will also decrease. However, this is not always possible in practice, the wall effect [2] becoming very important for H smaller than 0.5 mm.

For typical experimental conditions ($H = 10^{-3}$ m, $\Delta T_H = 0.2$ K) and physicochemical parameters characteristic of semiconductors ($\beta_T = 10^{-4}$ K^{-1}, $\nu = 3\times10^{-7}$ m^2 s^{-1}, D $= 10^{-8}$ m^2 s^{-1}), we find $Gr \times Sc = 66$. According to our numerical results, this would induce a mere 1% error, acceptable in most cases. For liquid metals, however, the diffusion coefficients are much smaller, of the order of $D = 2\times10^{-9}$ m^2 s^{-1}; the other parameters being held constant, we now have $Gr \times Sc = 333$ and the discrepancy would exceed 25%.

Larger capillaries or higher lateral temperature differences could thus lead to a catastrophic spread of the results and a careful design of the experimental set-up appears necessary. Even then, there is no guarantee that convective mass transport will not be significant, and obtaining a data bank with clean, reference diffusive measurements remains a challenge to the scientific community.

Such data could be obtained from microgravity experiments or, in the case of electrically conducting fluids, using a magnetic field in connection with a ground-based set-up. The Lorentz force is indeed known to significantly damp convective motion; the Hartmann number, $Ha = BH\ (\sigma/\eta)^{1/2}$ is the non-dimensional parameter scaling the intensity of the field [10], σ and η being, respectively, the electrical conductivity and the dynamic viscosity of the fluid.

At high Hartmann numbers, the velocity reduction is proportional to either Ha or Ha^2, depending on the geometry of the cavity [11, 12]. For values typical of metallic melts ($\sigma = 10^6\ \Omega^{-1}\mathrm{m}^{-1}$, $\eta = 2 \times 10^{-3}$ Pa s), a $B = 1$ T field in a cavity with $H = 10^{-3}$ m, would yield $Ha \simeq 22$. Some damping may then be expected, but the asymptotic regime would not be reached [11]; this means that higher field intensities could prove necessary in order to get rid of convective effects.

VI. CONCLUDING REMARKS

We used a coupled numerical/scaling analysis approach to gain some understanding of the effect of natural convection in diffusion coefficient measurement experiments. Both techniques lead to similar results and thus support each other. We observed that 'correct looking' profiles at the end of a simulated experiment and lateral segregation are not good indicators of convective interference; instead, the relevant criterion featured the square of the fluid velocity.

Of course, it should be kept in mind that our two-dimensional planar configuration may not be sufficient to adequately describe all the transport phenomena in an actual, cylindrical cell. However, we strongly believe that the main conclusions of this paper would stand, regardless of the degree of sophistication of the numerical simulations (see ref. [13] for a related question).

It can thus be stated that the design of an experimental set-up should be optimized, specially for species with low diffusion coefficients, such as liquid metals. In any case, carefully designed reference microgravity measurements would certainly be useful, as well as ground based experiments performed under intense magnetic fields.

Further work on this topic will feature the study of concentrated alloys, in order to clarify the interaction of the solutal and hydrodynamic fields. It would also be interesting to check the effect of a misalignment of the capillary with gravity and to perform a few three-dimensional simulations in more realistic configurations to assess the limitations of our simple model.

Acknowledgements—The present work was carried out in the frame of the GRAMME agreement between the Centre National d'Etudes Spatiales and the Commissariat à l'Energie Atomique, with financial support from the European Space Agency (ESTEC purchase order no. 135 095). J. P. Garandet would like to thank his friends J., F., Z. and O. for their help in improving the presentation of the manuscript. Numerous fruitful discussions on the topic with Drs G. Müller Vogt and J. P. Praizey are also gratefully acknowledged. The authors are indebted to Mr P. Dusserre for the preparation of the drawings.

REFERENCES

1. T. Iida and R. L. Guthrie, *The Physical Properties of Liquid Metals*, Chap. 7. Clarendon Press, Oxford (1993).
2. G. Frohberg and Y. Malmejac, Mass transport by diffusion. In *Fluid Sciences and Material Science in Space* (Edited by H. U. Walter), Chap. 5. Springer, Berlin (1987).
3. J. P. Praizey, Benefits of microgravity for measuring thermotransport coefficients in liquid metallic alloys, *Int. J. Heat Mass Transfer* **32,** 2385–2401 (1989).
4. G. Frohberg, K. H. Kraatz and H. Wever, Self diffusion of Sn^{112} and Sn^{124} in liquid tin, *Proc. 5th European Symp. Materials Science in Microgravity*, ESA SP-222, 201–205 (1984).
5. A. Bejan, *Convection Heat Transfer*, Chap. 4. Wiley, New York (1984).
6. J. P. Garandet, A. Rouzaud, T. Duffar and D. Camel, Comparison between order of magnitude and numerical estimates of the solute boundary layer in an idealised horizontal Bridgman configuration, *J. Crystal Growth* **113,** 587–592 (1991).
7. J. P. Garandet, Convection related radial segregation in an idealized horizontal Bridgman configuration: the quasi-diffusive regime limit, *J. Crystal Growth* **125,** 112–120 (1992).
8. R. V. Birikh, Thermocapillary convection in an horizontal layer of liquid, *J. Appl. Mech. Tech. Phys.* **3,** 69–72 (1966).
9. J. E. Hart, Low Prandtl number convection between differentially heated end walls, *Int. J. Heat Mass Transfer* **26,** 1069–1074 (1983).
10. R. Moreau, *Magnetohydrodynamics*, Chap. 4. Kluwer Academic, Dordrecht (1990).
11. J. P. Garandet, T. Alboussiere and R. Moreau, Buoyancy driven convection in a rectangular enclosure with a transverse magnetic field, *Int. J. Heat Mass Transfer* **35,** 741–748 (1992).
12. T. Alboussiere, J. P. Garandet and R. Moreau, Buoyancy driven convection with a uniform magnetic field. Part I: asymptotic analysis ($Ha \gg 1$), *J. Fluid Mech.* **253,** 545–563 (1993).
13. P. Bontoux, B. Roux, G. H. Schiroky, B. L. Markham and F. Rosenberger, Convection in the vertical mid plane of a horizontal cylinder. Comparison of two-dimensional approximations with three-dimensional results, *Int. J. Heat Mass Transfer* **29,** 227–240 (1986).

APPENDIX

Our purpose here is to estimate the integral of the convective term in equation (1). Since we do have to take into account the lateral variations of the axial concentration gradient, let us write:

$$G_R = \frac{2}{H}\int_{H/2}^{H} \partial C/\partial Z \, dX \quad G_L = \frac{2}{H}\int_{0}^{H/2} \partial C/\partial Z \, dX \tag{A1}$$

G_R and G_L stand for the average composition gradient along the Z-axis, respectively in the right and left parts of the cavity. We now define:

$$\bar{W} = \frac{2}{H}\int_{H/2}^{H} W \, dX = -\frac{2}{H}\int_{0}^{H/2} W \, dX \tag{A2}$$

as the average fluid velocity, positive with our choice of coordinate axes and temperature boundary condition. The integral of the convective contribution can then be, for order of magnitude purposes, written as:

$$\int_0^H W \partial C/\partial Z \, dX = \bar{W}(G_R - G_L)\frac{H}{2}. \tag{A3}$$

Let us suppose for instance that $C_0 > C_1$; all the vertical concentration gradients are then negative with our choice of coordinate axes, but conversely—from the direction of fluid motion (see Fig. 1)—lateral segregation is always positive. In order to make an estimate of equation (A3), we now need a relation between $(G_R - G_L)$ and the maximum lateral concentration variation ΔC_H, expected at the mid-height of the cavity ($Z = L/2$).

To start with, let us remark that at the location $L/2-\bar{\delta}$, the lateral segregation can be written as:

$$\Delta C(Z \simeq L/2-\bar{\delta}) = \Delta C_H - (G_R - G_L)\bar{\delta}. \tag{A4}$$

Now, since $\bar{\delta}$ was defined as the length scale of established Z-axis concentration gradient, we can safely assume that around $Z \simeq L/2-\bar{\delta}$, lateral segregation is very small with respect to its value at $Z = L/2$ ($\Delta C(Z \simeq L/2-\bar{\delta}) \ll \Delta C_H$). Equation (A4) thus becomes:

$$G_R - G_L = \Delta C_H/\bar{\delta}. \tag{A5}$$

Had we considered the location $Z \simeq L/2+\bar{\delta}$ or the case $C_0 < C_1$, the sign may have been opposite, but the same arguments would have led to a relation similar to equation (A5).

The last step of the analysis consists in building a link between ΔC_H and the average convective velocity $\bar{W}$. To this end, let us first remark that at the cavity mid-height ($Z = L/2$), the time variations of the concentration field are very slow, since C always remains close to $C_0 + C_1/2$. An additional idea is that at $Z = L/2$, the Z-concentration profiles are almost linear. We can thus write $\partial C/\partial t$, $\partial^2 C/\partial Z^2 \ll \partial^2 C/\partial X^2$; moreover, in that region, we also have $\partial C/\partial Z \simeq \vec{G}$, and so equation (1) becomes:

$$D\,\partial^2 C/\partial X^2 = W(X)\vec{G}. \tag{A6}$$

The order of magnitude of $\partial C/\partial X$ is $\Delta C_H/H$, since the X-variations take place over a length scale H. If we now use the no-flux condition $\partial C/\partial X = 0$ in $X = 0$ and $X = H$, the second order derivative is expected to scale as:

$$\partial^2 C/\partial X^2 \simeq (\partial C/\partial X|_{H/2} - \partial C/\partial X|_0)/(H/2) \simeq 2\Delta C_H/H^2$$

$$0 < X < H/2$$

$$\partial^2 C/\partial X^2 \simeq (\partial C/\partial X|_H - \partial C/\partial X|_{H/2})/(H/2) \simeq -2\Delta C_H/H^2$$

$$H/2 < X < H.$$

From the definition of $\bar{W}$ as the average velocity in the cavity, equation (A6) then reduces to $2D\Delta C_H/H^2 = -\bar{W}\vec{G}$, keeping in mind that both $\partial^2 C/\partial X^2$ and $\bar{W}$ change sign around $X = H/2$, and we finally get:

$$\Delta C_H = -\bar{W}\vec{G}H^2/2D. \tag{A7}$$

ΔC_H thus scales linearly with the fluid velocity. In a related problem, i.e. the modeling of lateral segregation in crystal growth [7], a similar conclusion could be drawn. Please note that with our choice $C_0 > C_1$, ΔC_H is indeed positive since $\vec{G}$ is negative.

Finally, combining the results of equations (A3), (A5) and (A7), we get for the absolute value of the integral of the convection term in equation (1) around the locations $Z = L/2 \pm \bar{\delta}$:

$$\int_0^H W \partial C/\partial Z \, dX = \frac{1}{4}\frac{H^3\bar{W}^2}{D\bar{\delta}}|\vec{G}|.$$